

DEVELOPMENT OF A GENERIC ULTRASOUND VIBRO-ACOUSTIC IMAGING PLATFORM FOR TISSUE ELASTICITY AND VISCOSITY

YI WANG*, SIPING CHEN*, TIANFU WANG*, TING ZHOU*,
QIAOLIANG LI*, YI ZHENG[†] and XIN CHEN*[‡]

**School of Medicine, Shenzhen University
Shenzhen Key Laboratory of Biomedical Engineering
Shenzhen, China*

*[†]Department of Electrical and Computer Engineering
St. Cloud State University
St. Cloud, MN 56301, USA*

[‡]chen.xin@szu.edu.cn

Accepted 15 November 2011

Published 21 January 2012

Tissue elasticity and viscosity are always associated with pathological changes. As a new imaging method, ultrasound vibro-acoustic imaging is developed for quantitatively measuring tissue elasticity and viscosity which have important significance in early diagnosis of cancer. This paper developed an ultrasound vibro-acoustic imaging research platform mainly consisting of excitation part and detection part. The excitation transducer was focused at one location within the medium to generate harmonic vibration and shear wave propagation, and the detection transducer was applied to detect shear wave at other locations along shear wave propagation path using pulse-echo method. The received echoes were amplified, filtered, digitized and then processed by Kalman filter to estimate the vibration phase. According to the phase changes between different propagation locations, we estimated the shear wave speed, and then used it to calculate the tissue elasticity and viscosity. Preliminary phantom experiments based on this platform show results of phantom elasticity and viscosity close to literature values. Upcoming experiments are now in progress to obtain quantitative elasticity and viscosity *in vitro* tissue.

Keywords: Ultrasound vibro-acoustic imaging; platform; elasticity; viscosity; shear wave.

1. Introduction

Tissue elasticity (stiffness) is always associated with pathological changes.¹ Therefore, the extraction of tissue elasticity information has important significance for clinical diagnosis. Clinically, on the one hand, palpation is used to perceive the

stiffness of the lesion region, as a basis to distinguish between benign and malignant tumors. However, this method fails when lesion is at deep location or it is very small, and characterization of stiffness is lack of quantitative criteria. On the other hand, almost all the clinical diagnostic

imaging techniques (ultrasound, X-ray, CT, MRI) are mainly focused on human tissue and organ anatomy imaging but cannot provide information of tissue elasticity. However, the elasticity of human tissue varies over several orders of magnitude² and can well distinguish different pathological changes. Therefore, elasticity obtained by quantitative measurement can play an important role in the early diagnosis of cancer.

Many techniques have been proposed to measure tissue elasticity, these methods are mostly based on ultrasound elastography³ and magnetic resonance (MR) elastography.⁴ Compared to the high cost of MR elastography, ultrasound elastography is more convenient in clinical practice. According to the different tissue excitation or detection ways, many methods have been developed to image tissue elasticity, including shear wave elasticity imaging (SWEI),² acoustic radiation force impulse imaging (ARFI),⁵ supersonic shear imaging (SSI),⁶ ultrasound-stimulated vibro-acoustography (USVA)⁷ and so on. However, there are still many problems in these methods mentioned above. SWEI and ARFI cannot obtain quantitative tissue elasticity and using displacement as a replacement for elasticity. SSI requires super fast imaging, so it is not compatible with current color Doppler scanner. Meanwhile most of the current methods ignore the viscosity of tissue which also has important significance for clinical diagnosis, and it will result in deviation of the elasticity estimation without considering the tissue viscosity.

Shear wave dispersion ultrasound vibrometry (SDUV) quantitatively measures tissue elasticity and viscosity by estimating the shear wave propagation speed at different tissue vibration frequencies.⁸⁻¹⁰ For a homogeneous medium, the shear wave propagation speed can be expressed as:

$$c_s = \sqrt{2(\mu_1^2 + \omega_s^2 \mu_2^2) / (\rho(\mu_1 + \sqrt{\mu_1^2 + \omega_s^2 \mu_2^2}))}, \quad (1)$$

where c_s is the shear wave propagation speed, ω_s is angular frequency, ρ , μ_1 , μ_2 are the density, shear elasticity and shear viscosity of the medium. In another approach, the shear wave speed can be estimated by phase changes along the propagation path:

$$c_s = \omega_s \Delta r / \Delta \varphi_s, \quad (2)$$

where $\Delta \varphi_s$ is the phase change over propagation distance Δr . According to Eq. (2), once we

obtain the shear wave phase change over a certain propagation distance, we can calculate the shear wave speed in this specific frequency. And according to Eq. (1), shear wave speed at multiple frequencies can be used to estimate the shear elasticity and shear viscosity of the medium. Based on this principle, SDUV uses amplitude modulated (AM) ultrasound wave to generate tissue harmonic vibration and shear wave propagation, and pulse-echo method to detect shear wave propagation. As the shear wave signal is extremely weak, phase is estimated by Kalman filter in slow time. Experiments show that this approach can accurately estimate very small harmonic vibration. Therefore, SDUV is a highly sensitive and quantitative measurement method for tissue elasticity and viscosity.

In this paper, we developed an ultrasound vibro-acoustic imaging research platform. This is a generic platform. Based on this platform, we can do either SDUV or ARFI method, and we focused on SDUV in this study. We simulated the extraction of shear wave phase by Kalman filter to evaluate the accuracy of the phase estimation. Preliminary phantom experiments based on SDUV had been taken in this platform, and phantom elasticity and viscosity were quantitatively measured.

2. Platform Development

2.1. Hardware configuration

Based on SDUV, ultrasound vibro-acoustic imaging research platform diagram is shown in Fig. 1.

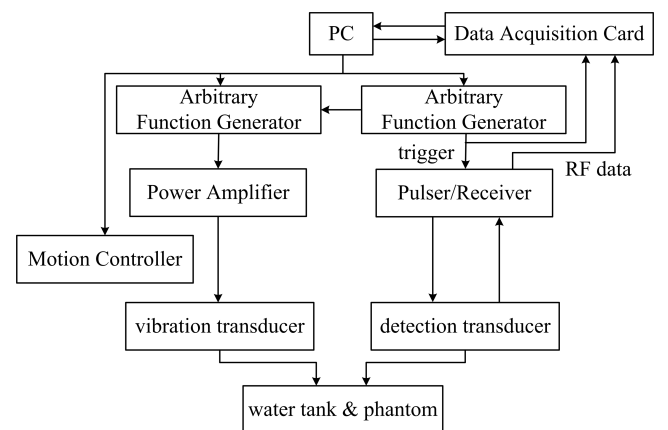


Fig. 1. Ultrasound vibro-acoustic imaging research platform diagram.

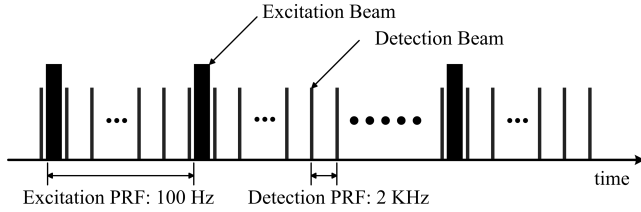


Fig. 2. Timing of the excitation beam and detection beam.

This platform mainly consists of excitation part and detection part: Amplitude modulation wave is generated by arbitrary function generator, and then amplified by the power amplifier (Gain 50 dB) to drive the excitation transducer; pulser/receiver drives the detection transducer and amplifies the ultrasound echo. The excitation transducer and detection transducer are fixed on three-axis stages. The transducers are focused on two locations with the same depths in the vertical direction.

In order to obtain shear wave propagation speed, phases of the vibration at different locations along the propagation path should be estimated to obtain the phase change over a propagation distance. Therefore, the timings of the excitation and detection beam of each detection location must be synchronized to validate the phase changes. The timing of the excitation and detection beams is shown in Fig. 2. The pulse repetition frequency (PRF) of excitation beam is 100 Hz, and PRF

of detection beam is 2000 Hz. In order to avoid interference, the excitation and detection beams are interleaved in the time domain. We achieve the synchronization by using another arbitrary function generator as the master trigger of the whole system. This master trigger stimulates the arbitrary function generator which generates excitation wave, pulser/receiver and data acquisition card simultaneously to ensure the synchronization of excitation beam, detection beam and A/D sampling.

The ultrasound vibro-acoustic imaging research platform is shown in Fig. 3. All the instruments on the platform are connected to the computer via their own interfaces. The control program is developed by LabVIEW.

2.2. Signal processing

The data processing program for estimation of vibration phase is developed by Matlab. Reference 9 gives a detailed derivation of estimation of vibration phase from consecutive echoes. The tissue motion induced by the excitation beam can be represented as:

$$d(t) = D \sin(\omega_s t + \varphi_s) \quad (3)$$

the vibration amplitude D and phase φ_s are random constants at a location. When detection pulses

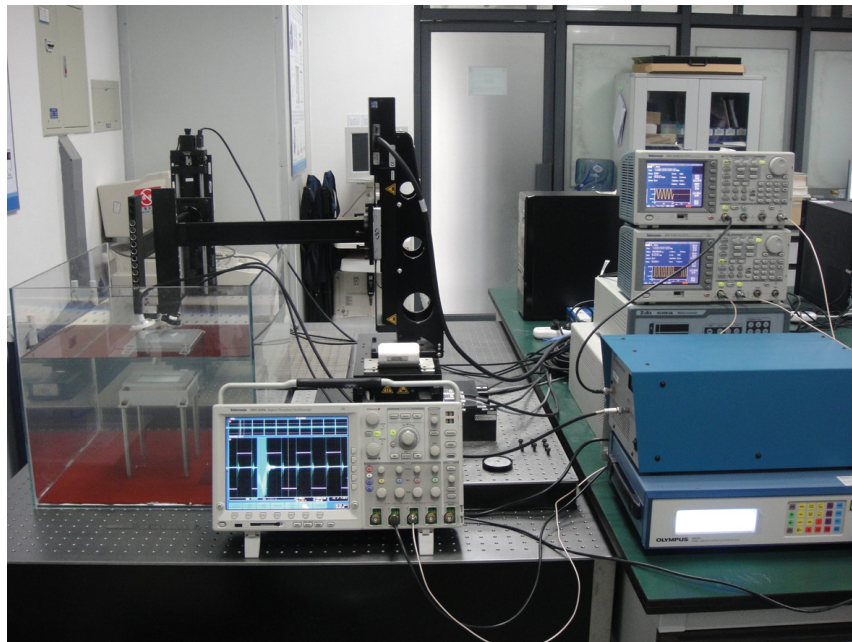


Fig. 3. Ultrasound vibro-acoustic imaging research platform.

separated by period T are applied to the vibration, the k th received echo is:

$$r(t, k) = |g(t, k)| \times \cos(\omega_0 t + \varphi_0 + \beta \sin(\omega_s(t + kT) + \varphi_s)), \quad (4)$$

where $\beta = 2D\omega_0 \cos(\theta)/c$, c is ultrasound speed, $g(t, k)$ is the complex envelope of $r(t, k)$, φ_0 is a transmitting phase constant and θ is the angle between the excitation and detection transducer. Then extracting the vibration using phase difference between two successive complex envelopes, the complex velocity quantity is obtained as:

$$\begin{aligned} v(t, k) &= X(t, k) + jY(t, k) = g(t, k)g^*(t, k + 1) \\ &= |g(t, k)||g(t, k + 1)| \\ &\quad \times \exp(j(\varphi(t, k) - \varphi(t, k + 1))), \end{aligned} \quad (5)$$

where the phase difference represents tissue vibration velocity. Extracting the phase difference, we have s signal:

$$\begin{aligned} s(t, k) &= -\tan^{-1}(Y(t, k)/X(t, k))/(2 \sin(\omega_s T/2)) \\ &= \beta \cos(\omega_s(t + kT) + \varphi_s + \omega_s T/2) \end{aligned} \quad (6)$$

it is a representation of tissue vibration velocity. Kalman filter uses s signal as its inputs to estimate tissue vibration.

3. Simulation and Phantom Experiment Results

3.1. Simulation of Kalman filter

In this paper, we used Field II to simulate the vibration of medium and the detection of echoes.

Then we used the Kalman filter to extract the shear wave phase to evaluate the accuracy of the phase estimate. Field II is an ultrasound program based on acoustic principles to simulate the ultrasound field generated by the probe. In Field II, we set the parameters as follow: The detection transducer had 5 MHz center frequency, 60% bandwidth, 2000 Hz PRF and 40 mm focal length. Tissue vibration amplitude was 1 μ m, frequency was 100 Hz, and duration was 10 periods. A/D sample rate was 100 MHz. Three detection locations were at the same depth but with an increment of 1 mm (phase increment of $\pi/6$) in the horizontal position. In the case of different signal to noise ratio (SNR), the phase changes estimated by 200 iterations of Kalman filter are shown in Table 1. As can be seen from the table, when there was no noise, the phase changes estimated by Kalman filter coincided with the theoretical value. With signal to noise ratio decreased until SNR = 10 dB, the estimation results were always good. Then when noise was equal or stronger than the signal, the deviation of the estimation results were relatively larger. And this result could be further improved by increasing the number of iterations of the Kalman filter. Table 2 demonstrates that the estimate of the phase changes can be improved by using 400 iterations of Kalman filter. Through the simulation results of the Kalman filter, we can see that Kalman filter can accurately estimate very small harmonic vibration and has high sensitivity of vibration phase estimation.

3.2. Phantom experiments

Experiment was conducted to quantitatively measure the elasticity and viscosity of gelatin phantom based on this research platform. The

Table 1. Phase changes estimated by Kalman filter with 200 iterations (Unit: rad).

Location	Phase change					Theoretical value
	SNR					
	No noise	30 dB	10 dB	0 dB	-3 dB	
Phase change between location 1 & 2	0.52	0.52	0.52	0.50	0.48	0.52
Phase change between location 2 & 3	0.52	0.52	0.52	0.58	0.55	

Table 2. Phase changes estimated by Kalman filter with 400 iterations (Unit: rad).

Location	Phase change					Theoretical value
	SNR					
	No noise	30 dB	10 dB	0 dB	-3 dB	
Phase change between location 1 & 2	0.52	0.52	0.52	0.52	0.53	0.52
Phase change between location 2 & 3	0.52	0.52	0.52	0.51	0.55	

excitation transducer had 1.03 MHz center frequency and 90 mm focal length. The detection transducer had 5.0 MHz center frequency and 40 mm focal length. The timing of excitation and detection beam is shown in Fig. 2. The excitation PRF is equal to 100 Hz and the detection PRF is equal to 2 KHz. Each excitation beam had an ultrasound frequency of 1.03 MHz and duration of $200 \mu\text{s}$ (duty ratio 2%). A/D sample rate was 100 MHz. The object vibrated by the ultrasound radiation force was a soldering bead (diameter about 1 mm) embedded in the gelatin phantom. Experiment setup in water tank is shown in Fig. 4. The excitation transducer (left) was focused on the soldering beam and the detection transducer (right) was focused on the position 1 mm away from the vibration center.

3.2.1. Phase estimation validation

We verified the accuracy of phase estimation. According to Eq. (2), we can see that the phase change is directly proportional to the time difference at a fixed location:

$$\Delta\varphi_s = \omega_s \Delta t. \quad (7)$$

We set the delay between excitation and detection beam as $470 \mu\text{s}$ and $440 \mu\text{s}$, respectively which induced the theoretical phase change of 0.02 rad according to Eq. (7). The measured phases at the position 1 mm away from the vibration center were -0.95 rad and -0.97 rad. The estimated phase change was 0.02 rad which coincided with the theoretical one. Therefore, the phase estimation of this method was accurate.

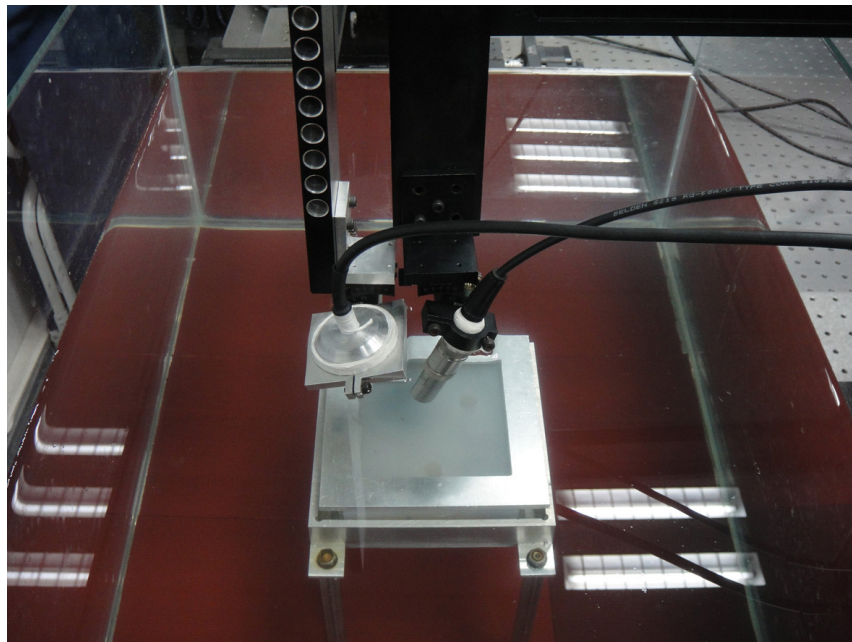


Fig. 4. Experiment setup in water.

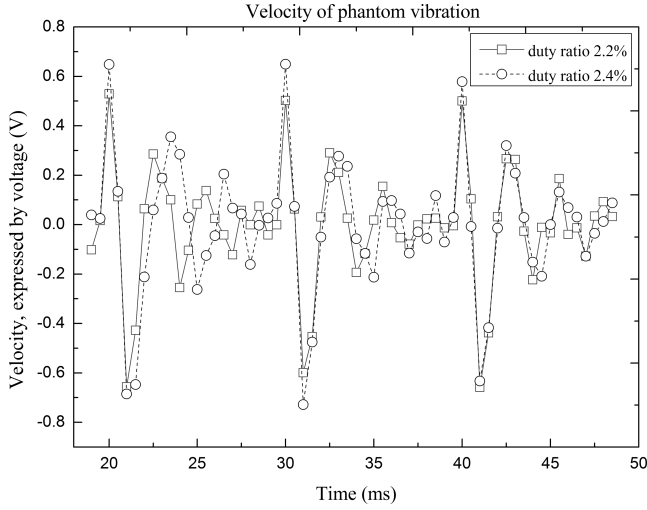


Fig. 5. Phantom vibration velocity of different pulse duration.

3.2.2. Tissue vibration velocity extraction

We made a comparison of s signal between different excitation duration. As mentioned earlier, s signal is a representation of tissue vibration velocity induced by ultrasound radiation force. Therefore, when the excitation duration is relatively longer, the tissue vibration velocity will be faster, and s signal is correspondingly larger. We used 2.2% and 2.4% duty ratio of excitation beam to push phantom, the s signal of different excitation duration is shown in Fig. 5. It can be seen when the excitation duration is longer, the phantom vibration velocity is faster.

3.2.3. Elasticity and viscosity estimation

We estimated the vibration phase of three locations. The three locations started at the position 1 mm away from the vibration center and separated with an increment Δr of 0.1 mm in the horizontal direction. The spectrum of our excitation beam contained the fundamental frequency of 100 Hz and harmonics of 200 Hz, 300 Hz, etc. The estimation for the harmonics can be done simultaneously by Kalman filter. Shear wave phase changes estimated by the Kalman filter are shown in Fig. 6, and the regressions of the estimated phase and regression errors are given in Table 3. Shear wave speed at multiple frequencies shown in Table 3 were brought in Eq. (1) to solve the elasticity and viscosity of gelatin phantom. The results were $\mu_1 = 1.76 \pm 0.06$ kPa, $\mu_2 = 0.55 \pm 0.12$ Pa·s.

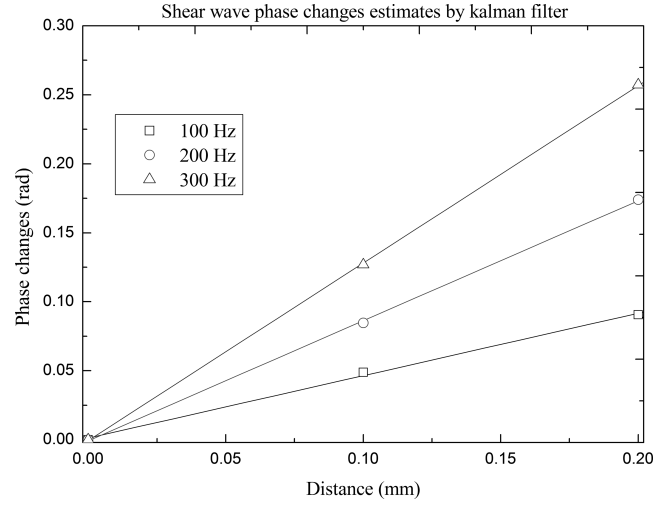


Fig. 6. Shear wave phase changes estimates by Kalman filter.

4. Discussion and Conclusion

In this paper, we developed a generic ultrasound vibro-acoustic imaging research platform. Based on this platform, we can do either SDUV or ARFI research. The entire platform is highly flexible and can automatically measure the elasticity and viscosity at one location very quickly. This fast acquisition makes multiple locations measurement in a relatively short time, leading to high efficiency and resolution. And for *in vivo* measurement, this rapid measurement can effectively avoid the impact of cardiac activity.

The experiment was conducted to quantitatively measure the elasticity and viscosity of gelatin phantom based on this research platform, and the measurement results of phantom elasticity and viscosity were $\mu_1 = 1.76 \pm 0.06$ kPa, $\mu_2 = 0.55 \pm 0.12$ Pa·s, respectively. Currently there is no gold standard for tissue elasticity and viscosity measurements. Our results are close to those reported in another gelatin phantom study: $\mu_1 = 2.22 \pm 0.08$ kPa, $\mu_2 = 0.24 \pm 0.03$ Pa·s,⁸ and in most literatures, μ_1 is always about 2 kPa, meanwhile, μ_2 is about 1 Pa·s.

Table 3. Phase change estimates and shear wave speed.

Vibration frequency (Hz)	Phase changes (rad)	Shear wave speed (m/s)
100	0.05 ± 0.01	1.40 ± 0.16
200	0.09 ± 0.01	1.45 ± 0.05
300	0.13 ± 0.01	1.47 ± 0.03

In our upcoming experiments, we expect to obtain quantitative elasticity and viscosity *in vitro* tissue. Due to the fast attenuation of ultrasound within tissue, the measurement depth becomes a major problem. With the increase of the depth, the ultrasound intensity will decay rapidly and may not generate sufficient tissue vibration. In our current platform, the excitation power could not generate sufficient vibration at deep location of medium, and this is the main limitation of our platform. We consider replacing the 50 dB power amplifier with 53 dB power amplifier to increase the excitation power in our upcoming experiments.

As the shear wave generated by tissue vibration is very weak and decays fast, it becomes a very critical problem to accurately characterize and detect the tissue vibration. In our future work, on the one hand, we expect to introduce coded ultrasound in detection part in order to improve the SNR of extracted vibration signal. On the other hand, we expect to optimize the Kalman filter in order to make a more accurate phase estimation.

Acknowledgments

This work was supported by the National Natural Science Foundation of China (Grant No. 81000637), the Key Program of National Natural Science Foundation of China (Grant No. 61031003), Shenzhen-HK innovative circle project (Grant No. ZYB200907090125A).

References

1. Y. C. Fung, *Biomechanics: Mechanical Properties of Living Tissues*, Springer-Verlag, New York (1993).
2. A. P. Sarvazyan, O. V. Rudenko, S. D. Swanson, J. B. Fowlkes, S. Y. Emelianov, "Shear wave elasticity imaging: A new ultrasonic technology of medical diagnostics," *Ultrasound Med. Biol.* **24**(9), 1419–1435 (1998).
3. J. Ophir, I. Cespedes, H. Ponnekanti, Y. Yazdi, X. Li, "Elastography: A quantitative method for imaging the elasticity of biological tissues," *Ultrason. Imag.* **13**, 111–134 (1991).
4. R. Muthupillai, D. J. Lomas, P. J. Rossman, J. F. Greenleaf, A. Manduca, R. L. Ehman, "Magnetic resonance elastography by direct visualization of propagating acoustic strain waves," *Science* **269**, 1854–1857 (1995).
5. K. Nightingale, M. S. Soo, R. Nightingale, G. Trahey, "Acoustic radiation force impulse imaging: *In vivo* demonstration of clinical feasibility," *Ultrasound Med. Biol.* **28**, 227–235 (2002).
6. J. Bercoff, M. Tanter, M. Fink, "Supersonic shear imaging: A new technique for soft tissue elasticity mapping," *IEEE Trans. Ultrason., Ferroelectr., Freq. Control* **51**(4), 396–408 (2004).
7. M. Fatemi, J. F. Greenleaf, "Ultrasound-stimulated vibro-acoustic spectrography," *Science* **280**, 82–85 (1998).
8. S. Chen, M. Fatemi, J. F. Greenleaf, "Quantifying elasticity and viscosity from measurement of shear wave speed dispersion," *Acoust. Soc. Am.* **115**(6), 2781–2785 (2004).
9. Y. Zheng, S. Chen, W. Tan, R. Kinnick, J. F. Greenleaf, "Detection of tissue harmonic motion induced by ultrasonic radiation force using pulse-echo ultrasound and Kalman filter," *IEEE Trans. Ultrason. Ferroelectr., Freq. Control* **54**(2), 290–300 (2007).
10. S. Chen, M. W. Urban, C. Pislaru, R. Kinnick, Y. Zheng, A. Yao, J. F. Greenleaf, "Shearwave dispersion ultrasound vibrometry (SDUV) for measuring tissue elasticity and viscosity," *IEEE Trans. Ultrason., Ferroelectr., Freq. Control* **56**(1), 55–62 (2009).